01 Jan 2017

Aerodynamic Design of the RAE 2822 in Transonic Viscous Flow: Single- and Multi-Objective Optimization Studies

Anand Amrit

Xiaosong Du
Missouri University of Science and Technology, xdnwp@mst.edu

Andrew Thelen

Leifur Leifsson

et. al. For a complete list of authors, see https://scholarsmine.mst.edu/mec_aereng_facwork/4918

Recommended Citation

A. Amrit et al., "Aerodynamic Design of the RAE 2822 in Transonic Viscous Flow: Single- and Multi-Objective Optimization Studies," *35th AIAA Applied Aerodynamics Conference, 2017*, American Institute of Aeronautics and Astronautics, Inc., AIAA, Jan 2017.
The definitive version is available at https://doi.org/10.2514/6.2017-3751

AIAA AVIATION Forum
5-9 June 2017, Denver, Colorado
35th AIAA Applied Aerodynamics Conference

10.2514/6.2017-3751

Aerodynamic Design of the RAE 2822 in Transonic Viscous Flow: Single- and Multi-Objective Optimization Studies

Anand Amrit[1], Xiaosong Du[2], Andrew Thelen[3], and Leifur Leifsson[4]
Iowa State University, Ames, Iowa 50011

Slawomir Koziel[5]
Engineering Optimization & Modeling Center, Reykjavik University, Menntavegur 1, 101 Reykjavik, Iceland

This paper addresses a benchmark aerodynamic design problem proposed by the AIAA Aerodynamic Design Optimization Discussion Group: Drag minimization of the RAE 2822 in transonic viscous flow at a fixed lift coefficient with constraints on the pitching moment coefficient and the cross-sectional area. The single-objective optimization (SOO) problem is solved using surrogate-based optimization (SBO) with the surrogates constructed through output space mapping and variable-resolution Reynolds-Averaged Navier-Stokes computational fluid dynamics models. Improving the implementation of our search algorithms enabled us to obtain the SOO optimal design four times faster than in our prior work in terms of CPU time. To explore the design space in the vicinity of the SOO optimal design, the problem is recast as a multi-objective optimization (MOO) one by treating the drag and pitching moment coefficients as the objectives while fulfilling the given constraints on the lift coefficient and the cross-sectional area. The MOO algorithm yields the Pareto front of the two conflicting objective functions in close proximity of the design obtained by the SOO formulation in the feasible and infeasible space of the original SOO problem.

Nomenclature

A	=	cross-sectional area
C_d	=	drag coefficient
C_m	=	pitching moment coefficient
C_l	=	lift coefficient
C_p	=	pressure coefficient
c	=	low-fidelity model
c	=	chord length
f	=	high-fidelity model
l	=	lower bound
M_∞	=	Mach number
t	=	airfoil thickness
u	=	upper bound
x	=	design variables
δ	=	trust region radius

Abbreviations

MOO	=	multi-objective optimization
SBO	=	surrogate based optimization
SOO	=	single-objective optimization
SM	=	space mapping
cts	=	counts

[1] Graduate Student, Department of Aerospace Engineering, Student Member AIAA.
[2] Graduate Student, Department of Aerospace Engineering, Student Member AIAA.
[3] Graduate Student, Department of Aerospace Engineering, Student Member AIAA.
[4] Assistant Professor, Department of Aerospace Engineering, Senior Member AIAA.
[5] Professor, School of Science and Engineering, Senior Member AIAA.

I. Introduction

This paper presents the results of solutions to the benchmark aerodynamic design Case 2 (drag minimization of the RAE 2822 in transonic viscous flow) developed by the AIAA Applied Aerodynamics technical committee. The results are presented in a special session at the annual AIAA Aviation 2017 conference.

In our prior work[1,2], we attempted to solve the lift-constrained drag minimization of RAE 2822 in viscous flow using approximation-based surrogates[3] and physics based surrogate techniques[4]. In our first paper[1], we used multi-fidelity optimization with the space mapping[5] (SM) technique to solve the problem. High-fidelity computational simulations were carried out using FLUENT[6] with the hyperbolic mesh generator by Kinsey and Barth[7], whereas the viscous-inviscid analysis method in MSES[8] was used for the low-fidelity computations. The airfoil shapes were parameterized using PARSEC[9]. In the second paper[2], we attempted to solve the same two-dimensional cases using the multi-level optimization[10] technique. In our solutions, we used a family of low-fidelity models constructed using the hyperbolic mesh generator[7] and the Stanford University Unstructured[11] (SU^2) solver to optimize a high-fidelity model by the same grid generator and flow solver as the low-fidelity models but with a higher mesh resolution (fully grid-independent solutions). In the third paper[12], we attempted to solve the problem using multi-fidelity techniques and improved computational models along with new correction technique. The paper demonstrated that multi-fidelity optimization with physics-based models can solve the two-dimensional case much faster than direct optimization with adjoint sensitivity information (see, e.g., Jameson[13]), and surrogate-based optimization[2] (SBO) with data-driven surrogate models[3]. Although the cost of multi-fidelity optimization is much lower, those techniques have so far not able to produce quality designs.

In this paper, we re-attempt to solve the two-dimensional aerodynamic design problem using an improved optimization framework and computational models. We use a hyperbolic mesh generator to generate the computational grid and solve the Reynolds-averaged Navier-Stokes (RANS) equations and the Spalart-Allmaras turbulence model[14] with the SU^2 solver[11]. The single-objective optimization (SOO) problem is solved using a multi-fidelity optimization approach with SM[5]. The problem is recast as a multi-objective optimization (MOO) problem by minimizing the drag coefficient and minimizing/maximizing the pitching moment coefficient for a fixed lift coefficient and with a constraint on the cross-sectional area. The multi-objective problem is solved using a surrogate-assisted MOO algorithm[4]. It involves the construction of local approximation models[3] along with multi-fidelity models to efficiently search the design space for Pareto optimal solutions.

The paper is organized as follows. Section II describes the general aerodynamic shape optimization problem formulation. Sections III, IV, and V give the detailed optimization method, computational models, and optimization results of benchmark case 2. The paper ends with conclusions.

II. Problem Formulation

The section describes the single- and multi-objective optimization problem formulations for benchmark case 2.

A. Single-Objective Optimization (SOO)

The aerodynamic design problem considered in this work involve lift-constrained drag minimization of airfoils in two-dimensional transonic flow. The objective here is to minimize the drag coefficient (C_d) of the RAE 2822 at a free-stream Mach number of $M_\infty = 0.734$, lift coefficient of 0.824, and Reynolds number of 6.5×10^6 subject to an area and pitching moment constraint. The constrained optimization problem can be expressed as:

$$\min_{\mathbf{l} \le \mathbf{x} \le \mathbf{u}} C_d \,, \tag{1}$$

subject to

$$C_l = 0.824, \tag{2}$$

$$C_m \ge -0.092, \tag{3}$$

$$A \ge A_{baseline}, \tag{4}$$

where C_m is the moment coefficient, and A is the airfoil cross-sectional area non-dimensionalized with the chord length squared.

B. Multi-Objective Optimization (MOO)

The objective is to find the trade-offs between the conflicting objectives, drag coefficient (C_d) and pitching moment coefficient (C_m) of the RAE 2822 at a free-stream Mach number of M_∞ = 0.734, lift coefficient of 0.824, and Reynolds number of 6.5×10^6 subject to an area and pitching moment constraint. We want to explore the designs in both feasible and infeasible regions as shown in Fig. 1 while satisfying the area constraint at a constant lift coefficient. The multi-objective constrained optimization problem can be expressed as:

Determine the Pareto Front in the Feasible Region:

$$\min_{l \le x \le u} C_d, \ \max_{l \le x \le u} C_m \tag{10}$$

subject to

$$C_l = 0.824, \tag{11}$$

$$C_m \ge -0.092, \tag{12}$$

$$A \ge A_{baseline}, \tag{13}$$

Determine the Pareto Front in the Infeasible Region:

$$\min_{l \le x \le u} C_d, \ \min_{l \le x \le u} C_m \tag{14}$$

subject to

$$C_l = 0.824, \tag{15}$$

$$C_m \le -0.092, \tag{16}$$

$$A \ge A_{baseline}, \tag{17}$$

III. Optimization Approaches

The section describes about the SOO and MOO approaches used to solve the problems defined in Sect. II.

A. Single-Objective Optimization (SOO)

The benchmark case is solved using a multi-fidelity approach with trust regions. Space mapping (SM)[5] algorithm as discussed in our previous paper[12], is utilized to perform SOO. Instead of executing the single objective optimization on the expensive high-fidelity model **f**, a cheap physics based surrogate model is utilized. The algorithm begins with

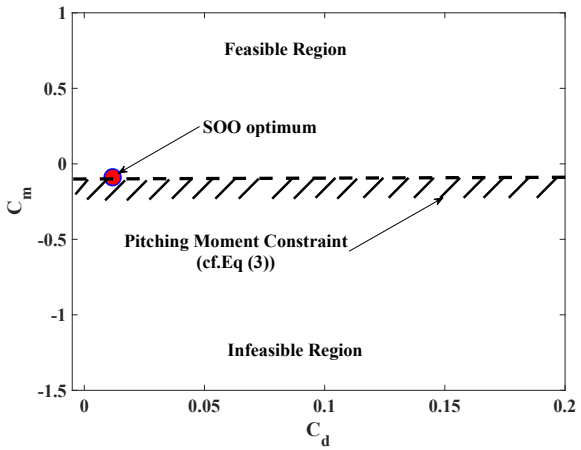

Figure 1. Illustration of the feasible and infeasible regions for design exploration.

evaluating the low and high-fidelity models of the baseline airfoil which is utilized in constructing the SM correction factor. The construction of these multi-fidelity models is described in section IV. The surrogate model is constructed by adding the correction factor to the low-fidelity model which elevates it to that of high-fidelity model. A well-known MATLAB optimizer, Fmincon is used, which finds the optimum. Optimization of the linear model is constrained to the vicinity of the current design defined as $\|\mathbf{x} - \mathbf{x}^{(i)}\| \leq \delta^{(i)}$, with the trust region radius $\delta^{(i)}$ adjusted adaptively using the standard trust region rules[20]. The termination conditions for the algorithm are: (i) $\|\mathbf{x}^{(i)} - \mathbf{x}^{(i-1)}\| < \varepsilon_x$, (ii) $|H^{(i)} - H^{(i-1)}| < \varepsilon_H$, (iii) $\delta^{(i)} < \varepsilon_\delta$, where ε_x, ε_H, and ε_δ are user defined convergence tolerances. For direct optimization of the aerodynamics design benchmark problem, we use: $\varepsilon_x = 10^{-4}$, $\varepsilon_H = 10^{-5}$, and $\varepsilon_\delta = 10^{-6}$.

The constant lift coefficient constraint (2) is implicitly satisfied within the flow solver by altering the angle of attack until the target lift is achieved. The pitching moment and cross-sectional area constraints (3) and (4), respectively, are handled directly through the optimizer.

B. Multi-Objective Optimization (MOO)

The aerodynamic design problem considered in this work is solved using a multi-objective approach. A data driven and multi-fidelity surrogate based optimization called the point-by-point method[15] is used to obtain the trade-offs between drag coefficient (C_d) and pitching moment coefficient (C_m). This method reaches to the Pareto front straight and moves along it point by point. The optimum drag coefficient (C_d) value, obtained using SOO approach is used as the starting point for the Point-by-point approach. A local appproximation model based on multi-fidelity surrogate is constructed to optimize the drag coefficient (C_d) while trying to reach a target pitching moment coefficient (C_m) value. The algorithm traverses in the feasible and in the infeasible regions to obtain a set of optimal solutions. The solution of the algorithm (10) and (14) is carried out using MATLAB's fmincon algorithm[17]. Fmincon handles the target pitching moment constarint and the area constraint directly and the algorithm is executed untill convergence. The algorithm converges when the target pitching moment value is within a given tolerence value of $1e^{-4}$. The algorithm is run repeatedly to obtain points in the vicinity of the starting point.

IV. Computational Modelling

This section describes the computational fluid dynamics modeling, and airfoil shape parameterization.

A. Design Variables

The B-spline parameterization approach, described in Jie *et al.*[12], is used in this case to control the upper and lower surfaces of the airfoil. We use 8 control points, as shown in Fig. 2, where two are fixed at the leading- and trailing-edges, and the other ones, 4 for each surface, can move in the vertical direction. This yields 8 design variables. Based on a fit to the RAE2822, we set the x-locations of the free control points as: $\mathbf{X} = [\mathbf{X}_u; \mathbf{X}_l]^T$ = [0.0 0.15 0.45 0.80; 0.0 0.35 0.60 0.90]^T. The initial design variable vector is $\mathbf{x} = [\mathbf{x}_u; \mathbf{x}_l]^T$ = [0.0175 0.0498 0.0688 0.0406; -0.0291 -0.0679 -0.0384 0.0054]^T. The lower bound of $\mathbf{x}$ is set as $\mathbf{l}$ = [0.015 0.015 0.015 0.015; -0.08 -0.08 -0.08 -0.01]^T, and the upper bound is set as $\mathbf{u}$ = [0.08 0.08 0.08 0.08;-0.01 -0.015 -0.015 0.01]^T.

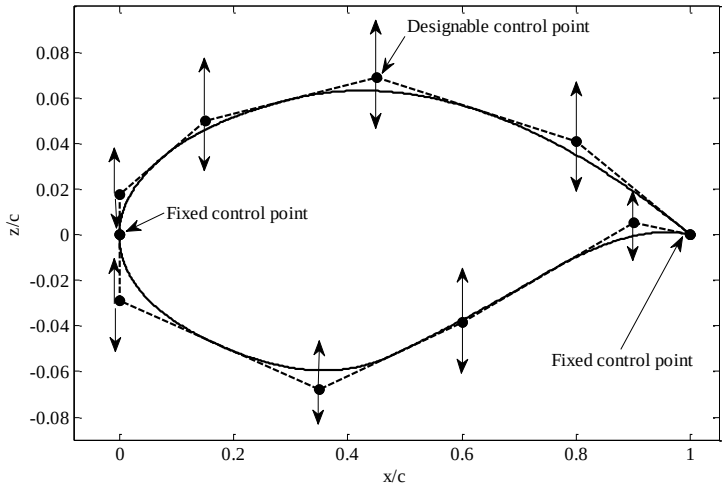

Figure 2. Airfoil shape parameterization using B-spline curves for the upper and lower surfaces.

B. High-Fidelity Viscous Aerodynamics Model (f)

The SU[2] implicit density-based flow solver is used for the viscous case, solving the steady compressible Reynolds-averaged Navier-Stokes (RANS) equations with the Spalart-Allmaras turbulent model[14]. The convective flux will be calculated using the second order JST scheme[16]. One multi-grid level is used for solution acceleration. The turbulent variables are convected using a first-order scalar upwind method. The flow solver convergence criterion is the one that occurs first of the two: (i) the change in the drag coefficient value over the last 100 iterations is less than 10^{-5}, or (ii) a maximum number of iterations of 20,000 is met.

The grids are generated using the hyperbolic C-mesh of Kinsey and Barth[7] (see Fig. 3). The farfield is set 100 chords away from the airfoil surface. The grid points are clustered at the trailing edge and the leading edge of the airfoil to give a minimum streamwise spacing of $0.001c$, and the distance from the airfoil surface to the fist node is $10^{-5}c$. The grid density is controlled by the number of points in the streamwise direction, and the number of points in the direction normal to airfoil surface. We set the number of points in the wake region equal to the number in the normal direction. Table 1 gives the results of a grid convergence study using the RAE 2822 airfoil at $M = 0.734$ and $C_l = 0.824$. The constant lift condition is determined by internally changing the angle of attack within the flow solver. The simulation time presented in Table 1 gives the overall time to compute the constant lift condition.

For the optimization studies, we use Mesh 3 for the high-fidelity model **f**. Mesh 4 is the finest and the most accurate. The difference between meshes 3 and 4 is around 1.75 drag counts for the baseline shape. However, Mesh 4 is almost five times more expensive than Mesh 3, hence the latter was chosen as the high-fidelity model for this work.

C. Low-Fidelity Viscous Aerodynamics Model (c)

The model set up for low-fidelity model is same as that of high-fidelity model (**f**). As shown in Table 1, we use Mesh 1 for the low-fidelity model **c**. The low-fidelity model convergence criteria are set with the following values: (i) change in the drag coefficient value over the last 100 iterations is less than 10^{-4}, or (ii) the maximum number of iterations is set to 5,000. Figure 4(a) shows that the low-fidelity solver is converged well within 5,000-iteration limit, and Figure 4 (b) shows that the low-fidelity model is a good representation of high-fidelity one in terms of the pressure coefficient distributions.

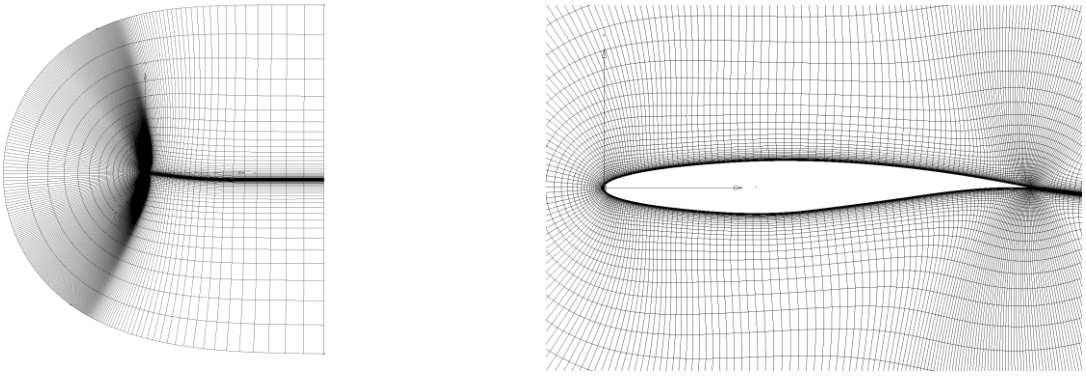

(a) **(b)**

Figure 3. Hyperbolic C-mesh used in the viscous model: (a) farfield view, (b) view close to the surface.

Table 1. Grid convergence study for the baseline shape of Benchmark Case 2.

Mesh	Grid Size	C_l (cts)	C_d(cts)	Simulation Time* (min)
1	9,836	0.824	324.6271	3.13
2	38,876	0.824	221.4551	8.79
3	154,556	0.824	204.7968	33.95
4	616,316	0.824	203.0495	152.62

* Computed on a high-performance cluster with 32 processors. Flow solution only.

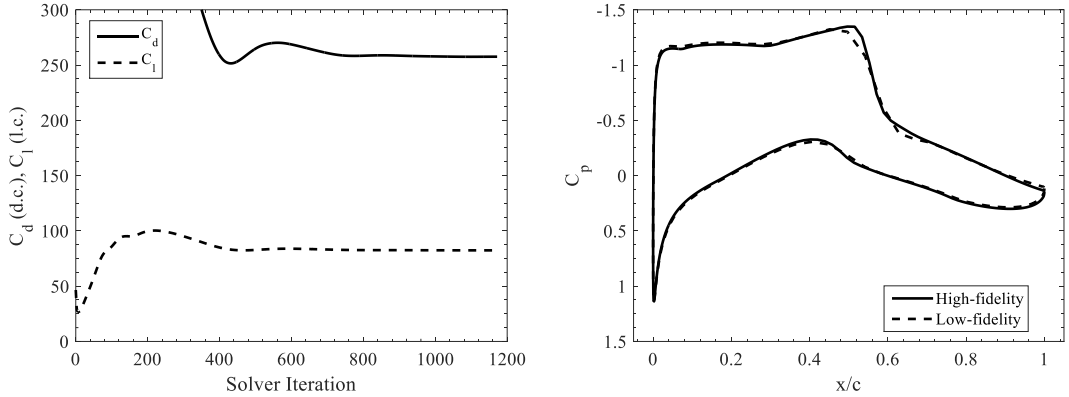

(a) **(b)**

Figure 4. Viscous flow simulation results for RAE 2822 at M = 0.734 and C_l = 0.824: (a) the evolution of the lift and drag coefficients obtained by the low-fidelity model, (b) a comparison of the pressure distributions obtained by the high- and low-fidelity models.

V. Results

This section describes the optimizations results of the single-objective and multi-objective optimization studies.

A. Single-Objective Optimization (SOO)

The SOO problem is solved using space mapping (SM) algorithm[5] and results are shown in Table 2. Figure 5(b). shows the convergence history of the algorithm indicating a considerable reduction in the objective function compared to that of the baseline airfoil. As can be seen in Table 2, the SM algorithm reduces the drag coefficient value from 203.80 cts to 119.49 cts. Figures 5(c) and (d) show comparisons of the shapes and pressure coefficient distributions of the baseline and SOO optimal designs. Figures 5(e) and (f) show the pressure coefficient contours of the baseline and optimum shape design respectively, indicating a considerable reduction of shock strength. In terms of number of function evaluations, SM based optimization utilized 423 low fidelity models and only 6 high fidelity models. The cost in terms of CPU time for the entire optimization process is approximately 19 hours on a HPC with 32 processors.

B. Multi-Objective Optimization (MOO)

The point-by point algorithm described in Koziel *et al.*[20], is utilized to perform the multi-objective optimization. The optimum drag value obtained from SOO, is utilized as the starting point for the algorithm. A target pitching moment value is then identified for the algorithm to attain while minimizing drag coefficient value. The runs are performed at M_∞ = 0.734 and A_{baseline} = 0.0779. The MOO algorithm needed one iteration to reach each target point. The cost of stepping from one point to another is approximately one hour. The total cost in terms of CPU time to obtain the entire Pareto is around 30 hrs on a HPC with 32 processors.

Figures 7(a) and (b) show the optimal solution set (Pareto front) obtained using MOO and a zoomed-in plot near SOO optimum respectively. The plots clearly reflect that; we cannot obtain any better optimum drag coefficient value other than SOO optimum. Few points (MOO Point 1 and MOO point 2) on the Pareto optimal set were selected to be compared with SOO optimum and the baseline design. Figures 7(c) and (d) show comparisons of all the airfoil shape designs and the pressure coefficient distributions for the selected points. There is not much difference in the pressure coefficient distribution compared to that of SOO optimum and that's because the selected points are near the optimum drag coefficient value.

Table 2. Single-objective optimization results.

Parameter/Method	Baseline	SPSO
C_l (l.c.)	82.35	82.40
C_d (d.c.)	203.80	119.49
$C_{m,c/4}$	-0.0905	-0.0919
A	0.0779	0.0779
N_c	–	423
N_f	–	6
CPU Time (hours)	–	19

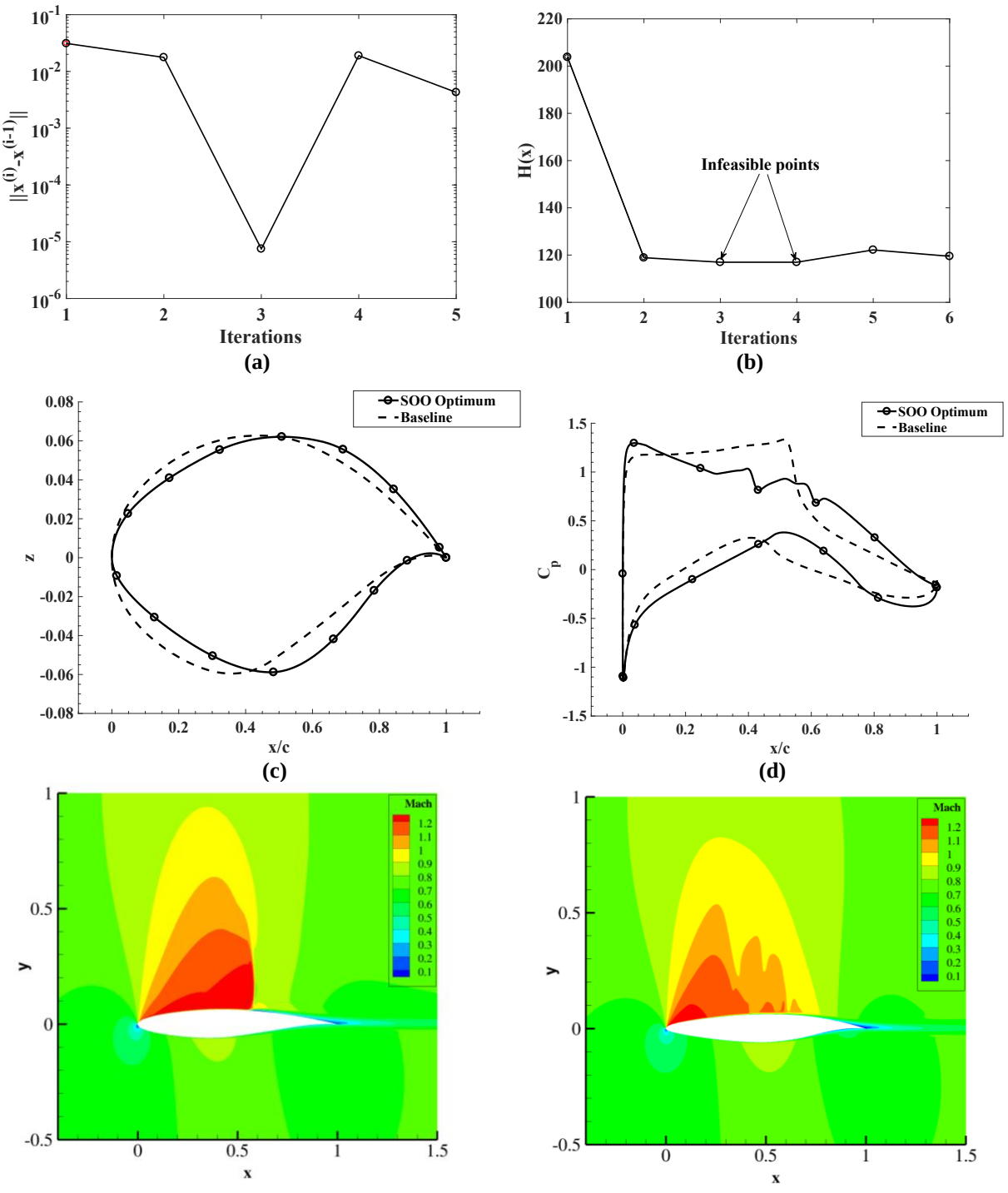

Figure 5. Single-objective optimization results: (a) convergence history of the arguments, (b) evolution of the objective function, (c) airfoil shape comparison, (d) pressure distribution comparison, (e) pressure coefficient contours of baseline airfoil, (f) pressure coefficient contours of optimum design from SOO.

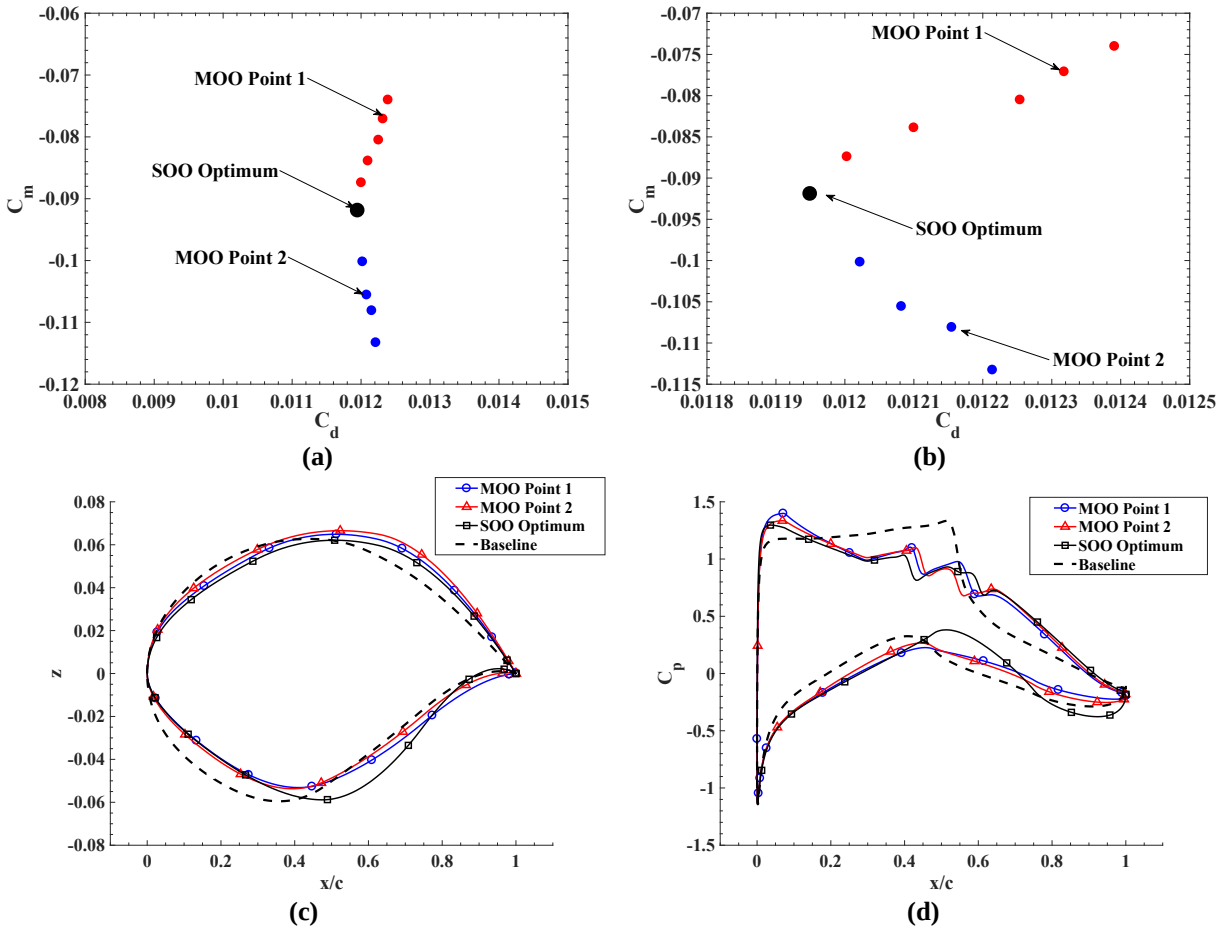

Figure 7. Multi-objective optimization results: (a) optimum solution set in feasible and infeasible regions, (b) zoomed-in plot of Fig. 7(a), (c) pressure distribution comparison, and (d) airfoil shape comparison.

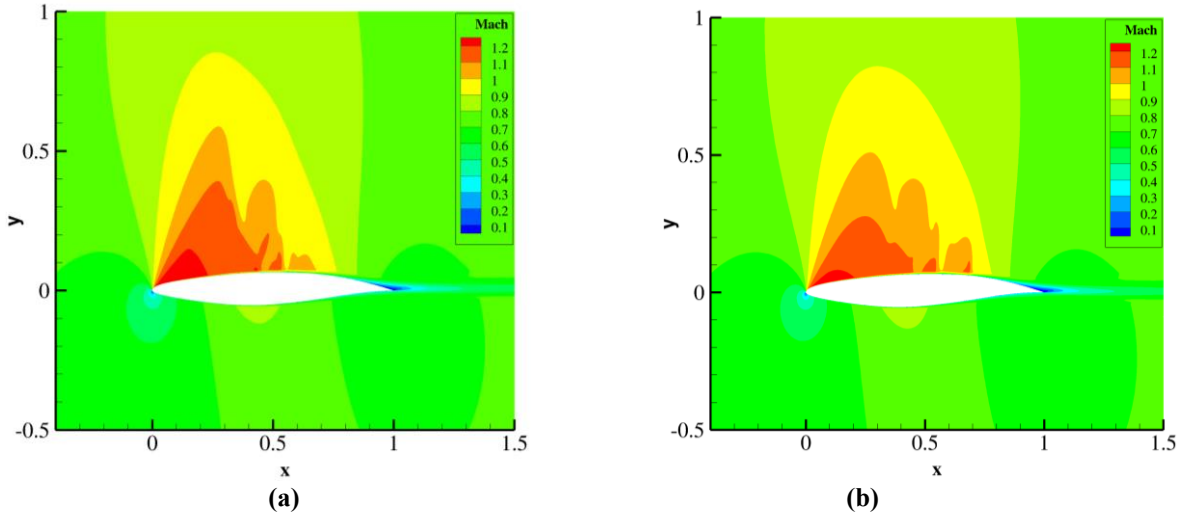

Figure 8. Pressure Coefficient Contours of (a) MOO point 1, (b) MOO point 2.

VI. Conclusion

The aerodynamic design benchmark case 2 has been solved using single-, and multi-objective optimization algorithms. Approximation-based and physics-based surrogate methods are utilized to accelerate the optimization procedure. Results from single-objective optimization (SOO) show a considerable reduction of total time utilized to obtain the optimum drag value compared to that of our previous work[12] due to improved implementations of the optimization algorithms and computational models. The vicinity of the SOO optimal design is explored in terms of the drag and pitching moment coefficients using a multi-objective optimization (MOO) algorithm.

References

[1]Leifsson, L., Koziel, S., Tesfahunegn, Y.A., Hosder, S., and Gramanzini, J.-R., "Aerodynamic Design Optimization: Physics-based Surrogate Approaches for Airfoil and Wing Design," *AIAA 52nd Aerospace Sciences Meeting*, National Harbor, Maryland, January 13-17, 2014.

[2]Tesfahunegn, Y.A., Koziel, A., Gramanzini, J.-R., Hosder, S., Han, Z.-H., and Leifsson, L., "Direct and surrogate-based optimization of benchmark aerodynamic problems: A Comparative Study," *53rd AIAA Aerospace Sciences Meeting, Science and Technology Forum*, Kissimee, Florida, Jan 5-9, 2015.

[3]A.I.J. Forrester and A.J. Keane, "Recent advances in surrogate-based optimization," *Prog. in Aerospace Sciences*, vol. 45, no. 1-3, pp. 50-79, Jan.-April, 2009.

[4]S. Koziel, D. Echeverría-Ciaurri, and L. Leifsson, "Surrogate-based methods," in S. Koziel and X.S. Yang (Eds.) *Computational Optimization, Methods and Algorithms*, Series: Studies in Computational Intelligence, Springer-Verlag, pp. 33-60, 2011.

[5]Koziel, S., and Leifsson, L., "Knowledge-based airfoil shape optimization using space mapping," AIAA Paper 2012-3016, 30th *AIAA Applied Aerodynamics Conference*, New Orleans, Louisiana, June 25-28, 2012.

[6]FLUENT, ver. 14.5.7, ANSYS Inc., Southpointe, 275 Technology Drive, Canonsburg, PA 15317, 2013.

[7]Kinsey, D. W., and Barth, T. J., "Description of a Hyperbolic Grid Generation Procedure for Arbitrary Two-Dimensional Bodies," AFWAL TM 84-191-FIMM, 1984.

[8]Drela, M., and Giles, M.B., "Viscous-Inviscid Analysis of Transonic and Low Reynolds Number Airfoils," *AIAA Journal*, vol. 25, no. 10, Oct. 1987, pp. 1347-1355.

[9]Sobieczky, H., "Parametric airfoils and wings," Recent developments of aerodynamic design methodologies, Braunschweig/Wiesbaden: Friedr. Vieweg & Sohn Verlagsgesellschaft mbH, 1999, pp. 71–87.

[10]Koziel, S., and Leifsson, L., "Multi-Level Surrogate-Based Airfoil Shape Optimization," 51st *AIAA Aerospace Sciences Meeting including the New Horizons Forum and Aerospace Exposition*, Grapevine, Texas, January 7-10, 2013.

[11]Palacios, F., Colonno, M. R., Aranake, A. C., Campos, A., Copeland, S. R., Economon, T. D., Lonkar, A. K., Lukaczyk, T. W., Taylor, T. W. R., and Alonso, J. J.**,** "Stanford University Unstructured (SU^2): An open-source integrated computational environment for multi-physics simulation and design," AIAA Paper 2013-0287**,** 51st *AIAA Aerospace Sciences Meeting and Exhibit*, Grapevine, Texas, USA, 2013.

[12]Ren, Z., Thelen, A. S., Amrit, A., Du, X., Leifsson, L., Tesfahunegn, Y.A., Koziel, S., "Application of Multifidelity Optimization Techniques to Benchmark Aerodynamic Design Problems", *54th AIAA Aerospace Sciences Meeting*, San Diego, California, USA.

[13]Jameson, A., "Aerodynamic Design via Control Theory," *Journal of Scientific Computing*, Vol. 3, 1988, pp. 233-260.

[14]Spalart, P. R. and Allmaras, S. R., "A One Equation Turbulence Model for Aerodynamic Flows", AIAA-Paper-92-0439, *38th AIAA Aerospace Sciences Meeting and Exhibit*, Reno, NV, January 6-9, 1992.

[15]Koziel, S., Bekasiewicz, A., "Rapid Multi-Objective Antenna Design Using Point-By-Point Pareto Set Identification," *IEEE Transactions of Antennas and Propagation*, vol. 64, no. 6, 2016.

[16]Jameson, A., Schmidt, W., and Turkel, E., "Numerical Solution of the Euler Equations by Finite Volume Methods Using Runge-Kutta Time-Stepping Schemes," AIAA 1981-1259, *AIAA 14th Fluid and Plasma Dynamic Conference*, Palo Alto, CA, June 23-25, 1981.

[17]MATLAB V15.0, Mathworks Inc., Corporate Headquarters, 3 Apple Hill Drive, Natick, MA 01760-2098, USA.